

# Perturbative approach to the penguin-induced $B \rightarrow \pi \phi$ decay

Blaženka Melić\*

*Theoretical Physics Division, Rudjer Bošković Institute, P.O. Box 1016, HR-10001 Zagreb, Croatia*

(Received 14 May 1998; revised manuscript received 19 October 1998; published 17 February 1999)

Using a modified perturbative approach that includes the Sudakov resummation and transverse degrees of freedom we analyze the penguin-induced  $B^- \rightarrow \pi^- \phi$  decay by applying the next-to-leading order effective weak Hamiltonian. The modified perturbative method enables us to include nonfactorizable contributions and to control virtual momenta appearing in the process. In addition, we apply the three-scale factorization theorem for nonleptonic processes that offers the possibility of having the scale-independent product of short- and long-distance parts in the amplitude of the weak Hamiltonian. The calculation supports the results obtained in the BSW factorization approach, illustrating the electroweak penguin dominance and the branching ratio of order  $\mathcal{O}(10^{-8})$ . However, the estimated prediction of 16% for the  $CP$  asymmetry is much larger than that obtained in the factorization approach. [S0556-2821(99)05605-2]

PACS number(s): 13.25.Hw, 12.38.Bx

## I. INTRODUCTION

Among a variety of heavy-meson decaying channels, exclusive two-body nonleptonic decays are theoretically the most challenging ones, owing to the phenomenon of hadronization and the effects of final-state interactions. On the other hand, they present the most promising way to detect  $CP$  violation in the heavy-meson sector and to explore the Cabibbo-Kobayashi-Maskawa (CKM) mixing matrix elements.

The mechanism of  $CP$  violation can be investigated directly in the charged sector of  $B$  mesons by measuring  $CP$  asymmetry.  $CP$  asymmetry is defined as the relative difference between the decay rates of the  $B$  meson and its  $CP$ -conjugated state: i.e.,

$$a_{CP} = \frac{\Gamma(B^- \rightarrow f) - \Gamma(B^+ \rightarrow \bar{f})}{\Gamma(B^- \rightarrow f) + \Gamma(B^+ \rightarrow \bar{f})}. \quad (1.1)$$

Nonvanishing  $CP$  asymmetries appear through the interference between amplitudes with different weak  $CP$ -violating phases and different  $CP$ -conserving strong phases coming from the final-state strong interactions different from zero.

Nowadays, experimental facilities offer a possibility of searching for  $CP$  asymmetries in penguin-induced nonleptonic decays, very promising decays to detect direct  $CP$  violation. Such decays have small branching ratios (BR), but satisfy both requirements for  $CP$ -violating asymmetry, owing to the fact that penguin diagrams are loop diagrams with different quark generations contributing with different weak  $CP$ -phases from the CKM matrix and that final-state strong interaction phases emerge from the absorptive part of penguin amplitudes. This mechanism of generating  $CP$  asymmetries in decays that involve penguin diagrams was first considered by Bander, Silverman, and Soni [1].

In this paper we discuss the pure penguin-induced  $B^- \rightarrow \pi^- \phi$  decay governed by the heavy-quark  $b \rightarrow ds\bar{s}$  decay. Performing a consistent  $1/N_c$  expansion ( $N_c$ , quark color

number) of QCD-penguin amplitudes, one can show that in this process the QCD-penguin contribution should be suppressed and the dominant contribution comes from the electroweak (EW)-penguin operators [2]. The  $B^- \rightarrow \pi^- \phi$  process has already been considered by many authors [3–6] within the Bauer-Stech-Wirbel (BSW) factorization approach [7]. This method for reducing the hadronic matrix element of four-quark operators to the product of two current-matrix elements cannot account for QCD interactions between the currents, except by parametrizing them by a phenomenological parameter in the generalized factorization approach [8]. In general, momenta of virtual gluons or photons in a process, appearing explicitly in the penguin matrix elements after factorization have to be considered free parameters.  $CP$  asymmetry depends strongly on these parameters and the predictive power of calculations performed within the factorization prescription is greatly reduced.

Our aim is to investigate the  $B^- \rightarrow \pi^- \phi$  decay in the modified perturbative approach. Perturbative calculations of exclusive  $B$  decays were carried out by different authors [9], all of them following the framework for analyzing exclusive decays in the perturbative QCD (PQCD) approach developed by Brodsky and Lepage, and other authors [10]. In the perturbative approach, exclusive amplitudes involving large momentum transfer factorize into a convolution of a process-independent and perturbatively incalculable distribution amplitudes (hadronic wave functions), one for each hadron involved into the decay, with a process-dependent and perturbatively calculable hard scattering amplitude of valence partons.

The applicability of such a PQCD framework to exclusive decays was widely discussed [11,12] owing to the concern about the possible uncontrollable nonperturbative (end-pion region) contributions and the problem was solved in a modified perturbative approach proposed by Li and Stermann [13].

Besides offering a reliable perturbative calculation, the modified perturbative approach offers a possibility of going beyond the factorization approximation in the calculation of four-quark matrix elements. It also enables us to assign the process-dependent virtual momenta  $q^2$  in the loop matrix elements and to fold them with their distribution in a particular decay. In this way, the uncertainties in  $CP$  asymmetry,

\*Email address: melic@thphys.irb.hr

which are due to some ad hoc quark model values of  $q^2$  as applied in the factorization approach, do not appear.

The purpose of this paper is to present a complete calculation of factorizable and nonfactorizable contributions in the penguin-induced  $B^- \rightarrow \pi^- \phi$  decay up to order  $\mathcal{O}(\alpha_s \alpha_{\text{em}})$ , testing the results on various CKM mixing matrix parameters. Especially, we wish to examine nonfactorizable contributions from the QCD-penguin operators and assign their role in the EW-penguin dominated processes, such as  $B^- \rightarrow \pi^- \phi$ .

The plan of the paper is as follows. In Sec. II we introduce the method of calculation based on the next-to-leading order (NLO) effective weak Hamiltonian, and the modified perturbative approach. A detailed analysis of the  $B^- \rightarrow \pi^- \phi$  process is presented in Sec. III. A discussion of mesonic wave functions and the Sudakov form factors is given in Sec. IV and the selection of proper mesonic wave functions is made. In Sec. V we present our numerical results for the branching ratio and  $CP$  asymmetry, comparing them with those obtained from the factorization approach and examine the dependence of the results on the choice of CKM parameters. Concluding remarks are given in Sec. VI.

## II. PERTURBATIVE MODEL FOR CALCULATING THE $B^- \rightarrow \pi^- \phi$ DECAY

The nonleptonic  $B^- \rightarrow \pi^- \phi$  decay is governed by the weak decay of the heavy  $b$ -quark,  $b \rightarrow ds\bar{s}$ . The light antiquark of the  $B$  meson is the spectator in the decay, being only slightly accelerated by the exchange of a hard gluon to form a pion in the final state.

In this section we present the basic ingredients for a calculation of such a penguin-induced decay. The first ingredient is the NLO effective weak Hamiltonian, which allows a consistent study of nonleptonic decays in which penguin operators are involved. The second ingredient, on which the paper is based, is a modified perturbative method for calculating exclusive decays by which the matrix elements of four-quark weak-Hamiltonian operators are perturbatively calculable.

### A. Low-energy effective weak Hamiltonian beyond the leading logarithmic approximation

Following Ref. [14] we consider the NLO effective weak Hamiltonian for  $b \rightarrow d$  transitions:

$$H_{\text{eff}}(\Delta B = -1) = \frac{G_F}{\sqrt{2}} \sum_{q=u,c} V_q \left( c_1(\mu) \mathcal{O}_1^{(q)} + c_2(\mu) \mathcal{O}_2^{(q)} + \sum_{k=3}^{10} c_k(\mu) \mathcal{O}_k \right). \quad (2.1)$$

The scale-dependent Wilson coefficients  $c_i(\mu)$  are the short-distance part of the Hamiltonian and include NLO QCD corrections and leading-order  $\alpha_{\text{em}}$  corrections. With  $V_q$  we denote products of CKM mixing matrix elements relevant to

$b \rightarrow d$  transitions,  $V_q = V_{qd}^* V_{qb}$ . Local four-quark operators, renormalized at the scale  $\mu$ , are

$$\begin{aligned} \mathcal{O}_1^{(q)} &= (\bar{d}_\alpha q_\beta)_{V-A} (\bar{q}_\beta b_\alpha)_{V-A}, \\ \mathcal{O}_2^{(q)} &= (\bar{d}q)_{V-A} (\bar{q}b)_{V-A}, \\ \mathcal{O}_3 &= (\bar{d}b)_{V-A} \sum_{q'} (\bar{q}'q')_{V-A}, \\ \mathcal{O}_4 &= (\bar{d}_\alpha b_\beta)_{V-A} \sum_{q'} (\bar{q}'_\beta q'_\alpha)_{V-A}, \\ \mathcal{O}_5 &= (\bar{d}b)_{V-A} \sum_{q'} (\bar{q}'q')_{V+A}, \\ \mathcal{O}_6 &= (\bar{d}_\alpha b_\beta)_{V-A} \sum_{q'} (\bar{q}'_\beta q'_\alpha)_{V+A}, \\ \mathcal{O}_7 &= \frac{3}{2} (\bar{d}b)_{V-A} \sum_{q'} e_{q'} (\bar{q}'q')_{V+A}, \\ \mathcal{O}_8 &= \frac{3}{2} (\bar{d}_\alpha b_\beta)_{V-A} \sum_{q'} e_{q'} (\bar{q}'_\beta q'_\alpha)_{V+A}, \\ \mathcal{O}_9 &= \frac{3}{2} (\bar{d}b)_{V-A} \sum_{q'} e_{q'} (\bar{q}'q')_{V-A}, \\ \mathcal{O}_{10} &= \frac{3}{2} (\bar{d}_\alpha b_\beta)_{V-A} \sum_{q'} e_{q'} (\bar{q}'_\beta q'_\alpha)_{V-A}, \end{aligned} \quad (2.2)$$

where  $V \pm A = 1/2 \gamma_\mu (1 \pm \gamma_5)$ ,  $\alpha$  and  $\beta$  are color indices,  $q' \in \{u, d, s, c, b\}$ , and  $e_{q'}$  are the corresponding quark charges.  $\mathcal{O}_1^{(q)}$  and  $\mathcal{O}_2^{(q)}$  are tree-level operators,  $\mathcal{O}_3, \dots, \mathcal{O}_6$  are QCD-penguin operators, and  $\mathcal{O}_7, \dots, \mathcal{O}_{10}$  are EW penguin operators.

From the quark content of the operators  $\mathcal{O}_1^{(q)}$  and  $\mathcal{O}_2^{(q)}$  it is obvious that they do not contribute at the tree level in  $b \rightarrow ds\bar{s}$  transitions. Such transitions are pure penguin-induced, receiving contributions from the operators  $\mathcal{O}_3, \dots, \mathcal{O}_{10}$ , in which  $q'$  is restricted to be a strange quark,  $q' = s$ .

In the NLO weak Hamiltonian (2.1) the renormalization-scheme dependence of the Wilson coefficients is explicitly canceled by the inclusion of the one-loop QCD and QED matrix elements of the tree-level operators  $\mathcal{O}_{1,2}^{(q)}$ , Fig. 1. The one-loop matrix elements of the NLO weak Hamiltonian for a  $b \rightarrow ds\bar{s}$  transition can be written in terms of products of the tree-level matrix elements of penguin operators and the renormalization scheme-independent coefficients  $\bar{c}(\mu)$ :

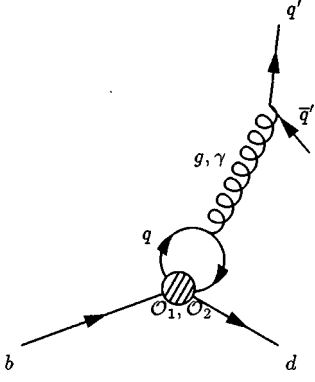


FIG. 1. QCD and QED one-loop penguinlike contributions of the tree-level operators  $\mathcal{O}_1$  and  $\mathcal{O}_2$  in the  $b \rightarrow dq' \bar{q}'$  decay.

$$\begin{aligned}
 & \langle ds\bar{s} | \mathcal{H}_{eff}(\Delta B = -1) | b \rangle \\
 &= \frac{G_F}{\sqrt{2}} \sum_{q=u,c} V_q \left( \sum_{k=3}^{10} \bar{c}_k(\mu) \langle \mathcal{O}_k \rangle^{\text{tree}} - \frac{\alpha_s(\mu)}{24\pi} \bar{c}_2(\mu) \right. \\
 & \quad \times \left\{ \left\langle \left( \frac{10}{9} - \Delta G(m_q^2, q^2, \mu^2) \right) \right. \right. \\
 & \quad \times (\mathcal{O}_3 - 3\mathcal{O}_4 + \mathcal{O}_5 - 3\mathcal{O}_6) \Bigg\rangle^{\text{tree}} \Bigg\} \\
 & \quad + \frac{\alpha_{\text{em}}}{9\pi} (3\bar{c}_1(\mu) + \bar{c}_2(\mu)) \\
 & \quad \times \left\{ \left\langle \left( \frac{10}{9} - \Delta G(m_q^2, q^2, \mu^2) \right) (\mathcal{O}_7 + \mathcal{O}_9) \right\rangle^{\text{tree}} \right\}, \quad (2.3)
 \end{aligned}$$

where  $\langle \mathcal{O}_k \rangle^{\text{tree}} = \langle ds\bar{s} | \mathcal{O}_k | b \rangle^{\text{tree}}$ .

The function  $\Delta G(m_q^2, q^2, \mu^2)$  arises from the one-loop penguinlike diagrams with  $q=u, c$  quarks in the loop:

$$\Delta G(m_q^2, q^2, \mu^2) = -4 \int_0^1 du u(1-u) \ln \left( \frac{m_q^2 - q^2 u(1-u)}{\mu^2} \right). \quad (2.4)$$

Here, as well as the quark mass  $m_q$  and the renormalization scale  $\mu$ , there appears a new parameter  $q^2$ , which is the momentum squared of a virtual gluon or photon emerging from the loop. In the  $b \rightarrow ds\bar{s}$  transition  $q^2$  can be identified with the sum of the strange quark momenta squared.

Concentrating now on the specific process  $B^-(b\bar{u}) \rightarrow \pi^-(d\bar{u})\phi(s\bar{s})$ , a few comments are in order. The strange quark and antiquark building  $\phi$ -meson are obviously in the color-singlet state. The  $s\bar{s}$  pair coming from the virtual gluon decay in the QCD-penguin diagrams builds a color-octet state. Therefore, first, one expects a small contribution from the QCD-penguin operators and, second, the one-loop QCD penguinlike contribution (shown in Fig. 1 with an exchanged

gluon) is not present in the  $B^- \rightarrow \pi^- \phi$  decay. The final expression for the matrix element is then

$$\begin{aligned}
 & \langle \pi^- \phi | \mathcal{H}_{eff}(\Delta B = -1) | B^- \rangle \\
 &= \frac{G_F}{\sqrt{2}} \sum_{q=u,c} V_q \left( \sum_{k=3}^{10} \bar{c}_k(\mu) \langle \mathcal{O}_k \rangle^{\text{tree}} \right. \\
 & \quad + \frac{\alpha_{\text{em}}}{9\pi} \left( \frac{10}{9} - \Delta G(m_q, \langle q^2 \rangle, \mu) \right) (3\bar{c}_1(\mu) \\
 & \quad + \bar{c}_2(\mu)) \{ \langle \mathcal{O}_7 \rangle^{\text{tree}} + \langle \mathcal{O}_9 \rangle^{\text{tree}} \} \Bigg). \quad (2.5)
 \end{aligned}$$

Here  $\langle \mathcal{O}_k \rangle^{\text{tree}} \simeq \langle \pi^- \phi | \mathcal{O}_k | B^- \rangle$ .

We have retained the  $\alpha_{\text{em}}$ -proportional term as a part of the NLO weak Hamiltonian, although we show later that, in the perturbative approach to the order we are working with, such a contribution emerges naturally. This term is producing hard final-state interaction phase shifts, necessary for generating  $CP$  asymmetry, which are due to the on-shell quarks rescattering in the loop for particular values of  $q^2$ . The  $CP$  asymmetry depends strongly on the value of  $q^2$  and, in the factorization approach, the major source of uncertainties in predictions comes from the lack of information about the  $q^2$  value after the factorization of hadronic matrix elements is performed. On the contrary, in the perturbative approach, the  $q^2$ -dependence of the loop amplitude is calculable directly as a part of the hadronic matrix element and it is determined by the momentum distributions in a particular process. However, in the strict factorization, and in the perturbative calculation for the process considered, the average  $q^2$ -value can be simply determined to be the mass of the  $\phi$  meson squared,  $\langle q^2 \rangle = M_\phi^2$ . Further discussion about this point is left for Sec. V.

Let us now continue with the estimation of the matrix elements of four-quark operators.

### B. Modified perturbative approach to the calculation of the matrix elements of four-quark operators

Perturbative calculations of matrix elements in exclusive hadron decays can be carried out in the Brodsky-Lepage (BL) formalism [10]. Hadrons are considered in the leading approximation as a bound state of valence quarks and/or antiquarks, depending on the hadron. The amplitude of the process factorizes into the convolution of distribution amplitudes of hadrons involved in the decay (hadron wave functions) and the hard scattering amplitude of valence partons. Hadronic wave functions represent the nonperturbative part, which has to be determined for heavy hadrons in relativistic constituent or nonrelativistic models, or for light hadrons by the QCD sum-rule method or by lattice calculations. Further discussion about the wave functions is given in Sec. IV.

The hard scattering amplitude can be calculated perturbatively, taking into account all possible exchanges of a hard gluon between valence partons in a given  $\alpha_s$ -order of the calculation. Valence quarks are carrying some fraction of

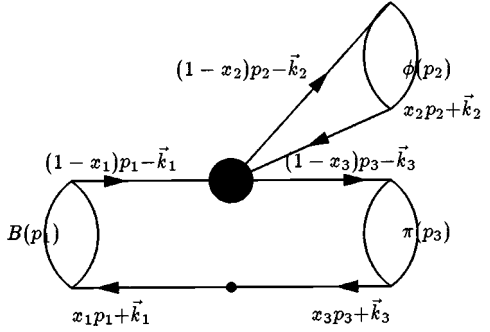


FIG. 2. The basic graph of the  $B^- \rightarrow \pi^- \phi$  decay with the momentum definitions specified. The black circle stands for the NLO effective weak Hamiltonian (2.1).

momentum of their parent hadron and the final expression is integrated over the fractions  $x_i$  ( $i=1,2,3$ ), see Fig. 2. The concern about the applicability of this method to exclusive processes was raised when it was noted that even at large momentum transfer the contribution to these processes could come predominantly from the momentum regions in which  $\alpha_s$  is large [11,12]. The problem is connected with the end-point region of momentum fractions. Namely, when one of the hadron constituents carries all the momentum of a hadron, the situation is no more perturbative and significant uncontrollable soft contributions might appear. The solution of the problem was proposed by Li and Sterman [13]. Contrary to the BL formalism, they suggested to go beyond the collinear approximation and to retain the small transverse momentum of valence quarks. Owing to the transverse degrees of freedom, the parton virtualities become large enough in the whole region for a reliable perturbative calculation. Furthermore, they included the Sudakov form factor for each of the hadrons in the decay to suppress the contributions from dangerous soft regions. All these effects can be incorporated into the factorization formula by expressing the transverse momentum variables in the Fourier transformed  $b$ -space.

The very last formula, which is used throughout this paper to calculate the matrix elements of four-quark operators from Eq. (2.5) relevant to the  $B^- \rightarrow \pi^- \phi$  decay, is

$$\begin{aligned} & \langle \pi^- \phi | \mathcal{O}_k | B^- \rangle \\ &= \int [dx] \int \left[ \frac{d^2 \vec{b}}{4\pi} \right] \Psi_\pi^*(x_3, \vec{b}_3) \Psi_\phi^*(x_2, \vec{b}_2) \\ & \quad \times T_k(\{x\}, \{\vec{b}\}, M_B) \Psi_B(x_1, \vec{b}_1) e^{-S(\{x\}, \{\vec{b}\}, M_B)}, \end{aligned} \quad (2.6)$$

where  $x_i$  ( $i=1,2,3$ ) are fractions of longitudinal momenta of  $B$ ,  $\phi$ , and  $\pi$  mesons, respectively. Analogously,  $b_i$  denote the Fourier-transformed transverse momenta of these mesons.  $[dx] = dx_1 dx_2 dx_3$  and  $\{x\}$  denotes the set of variables  $\{x_1, x_2, x_3\}$ . Similarly, for  $\vec{b}$  variables.  $\Psi_\pi^*$ ,  $\Psi_\phi^*$ , and  $\Psi_B$  are the wave functions of the outgoing  $\pi$  and  $\phi$  mesons, and the decaying  $B$  meson, respectively.  $T_k$  is the hard scattering amplitude describing the  $B \rightarrow \pi \phi$  decay at the one-loop level

caused by one of the operators  $\mathcal{O}_k$  (2.2). The exponential factor in formula (2.6) is the Sudakov factor. Its explicit form is given in Sec. IV.

### III. CALCULATION OF THE $B^- \rightarrow \pi^- \phi$ DECAY

The basic graph representing the  $B^- \rightarrow \pi^- \phi$  decay in the perturbative approach is shown in Fig. 2.

In order to perform the calculation, we have to specify the hadronic momenta. The simplest choice can be made using the light-cone coordinates and taking the  $B$  meson to be at rest:

$$P_B = p_1 = \frac{M_B}{\sqrt{2}}(1, 1, \vec{0}), \quad p_1^2 = M_B^2,$$

$$P_\phi = p_2 = \frac{M_\phi}{\sqrt{2}}(1, r^2, \vec{0}), \quad p_2^2 = M_\phi^2,$$

$$P_\pi = p_3 = \frac{M_B}{\sqrt{2}}(0, 1 - r^2, \vec{0}), \quad p_3^2 = 0. \quad (3.1)$$

Here,  $M_B$  and  $M_\phi$  are the masses of the  $B$  and the  $\phi$  meson, respectively, and  $r$  is defined as their ratio,  $r = M_\phi / M_B$ . The pion is taken to be massless. In addition to carrying some portion of the momentum of their parent meson, the valence quarks also carry some small transverse momentum  $\vec{k}$  (see Fig. 2).

Working in the leading order, the perturbative part, namely, the amplitudes of the four-quark operators (2.6), can be calculated from the Feynman graphs with all possible attachments of a hard gluon, shown in Fig. 3. As discussed later explicitly, Fig. 3(a) shows factorizable amplitudes of the decay. Figure 3(b) shows nonfactorizable amplitudes, not presented in the BSW-factorization approach. Contributions of one-loop induced penguinlike diagrams coming from the tree-level operators are shown in Fig. 3(c). These contributions can be taken into account immediately assuming the NLO weak Hamiltonian, but they emerge naturally in the perturbative model. Finally, Fig. 3(d) shows some additional diagrams that have to be included to perform a proper  $\mathcal{O}(\alpha_s \alpha_{\text{em}})$  calculation.

In full hadron wave functions one can split up spin wave functions from the rest; particularly,

$$\Psi_B(x_1, \vec{b}_1) = \frac{1}{\sqrt{2}} (\not{p}_1 + M_B) \gamma_5 \frac{\mathbb{1}_c}{\sqrt{3}} \Phi_B(x_1, \vec{b}_1),$$

$$\Psi_\phi^*(x_2, \vec{b}_2) = \frac{1}{\sqrt{2}} \not{\epsilon} (\not{p}_2 + M_\phi) \frac{\mathbb{1}_c}{\sqrt{3}} \Phi_\phi^*(x_2, \vec{b}_2),$$

$$\Psi_\pi^*(x_3, \vec{b}_3) = \frac{1}{\sqrt{2}} \gamma_5 \not{p}_3 \frac{\mathbb{1}_c}{\sqrt{3}} \Phi_\pi^*(x_3, \vec{b}_3), \quad (3.2)$$

where  $\mathbb{1}_c$  is the unit color matrix,  $\epsilon^\mu$  is the polarization vector of the  $\phi$  meson. The scalar wave functions  $\Phi$  are specific to each of the mesons and are discussed in Sec. IV.

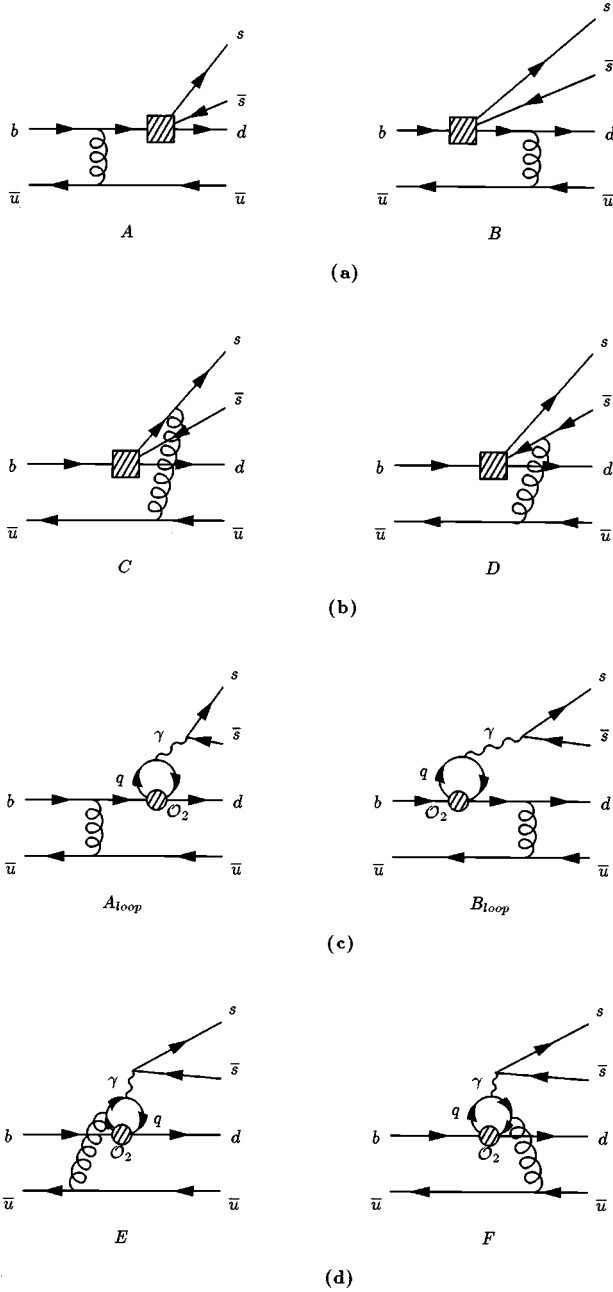


FIG. 3. Leading-order contributions to the  $B^- \rightarrow \pi^- \phi$  decay: (a) factorizable, (b) nonfactorizable, and (c) and (d) penguinlike. The square stands for the penguin operators  $\mathcal{O}_k$ ,  $k=3, \dots, 10$ , and the circle represents the tree-level operator  $\mathcal{O}_2$ .

In this process it is enough to calculate QCD-penguin contributions, because EW-penguin operators are simply related to QCD penguin operators as

$$\mathcal{O}_3 = (\bar{d}b)_{V-A}(\bar{s}s)_{V-A} = \frac{2}{3e_s}\mathcal{O}_9,$$

$$\mathcal{O}_4 = -(\bar{d}s)_{V-A}(\bar{s}b)_{V-A} = \frac{2}{3e_s}\mathcal{O}_{10},$$

$$\mathcal{O}_5 = (\bar{d}b)_{V-A}(\bar{s}s)_{V+A} = \frac{2}{3e_s}\mathcal{O}_7,$$

$$\mathcal{O}_6 = -2(\bar{d}s)_{S+P}(\bar{s}b)_{S-P} = \frac{2}{3e_s}\mathcal{O}_8, \quad (3.3)$$

where  $e_s$  is the strange quark charge,  $e_s = -1/3e$ .

Applying the standard procedure for calculating Feynman diagrams, the hard scattering amplitudes  $T_k$  can be easily worked out by performing color and spin traces. They appear after the spin and color parts of the wave functions are added to the amplitude, leaving the scalar functions  $\Phi$  at the place of the full mesonic wave functions  $\Psi$  in Eq. (2.6).

All operators receive the same contribution from the factorizable diagrams, Fig. 3(a):

$$T_{fact} = T_A + T_B,$$

$$T_A = -4\pi\alpha_s(\mu)C_f\frac{N_c}{\sqrt{3}}\frac{1}{2\sqrt{2}}32M_B^3r \times [(1+x_3(1-r^2))\epsilon \cdot p_3] \cdot \frac{1}{D_G} \frac{1}{D_b},$$

$$T_B = -4\pi\alpha_s(\mu)C_f\frac{N_c}{\sqrt{3}}\frac{1}{2\sqrt{2}}32M_B^3r \times [x_1(1-r^2)\epsilon \cdot p_1 - x_1\epsilon \cdot p_3] \cdot \frac{1}{D_G} \frac{1}{D_{q_1}}, \quad (3.4)$$

where  $C_f$  is the color factor equal to  $C_f = C_F = 4/3$  for the  $\mathcal{O}_3(\mathcal{O}_9)$  and  $\mathcal{O}_5(\mathcal{O}_7)$  operators and  $C_f = C_F/N_c$  for the others. We are going to take the number of colors  $N_c$  to be equal to 3.

$D_G$ ,  $D_b$ , and  $D_{q_1}$  denote the denominators of the exchanged gluon, and of the virtual  $b$  and  $d$  quark propagators, respectively:

$$D_G = q_G^2 + i\eta = M_B^2[x_1^2 - x_1x_3(1-r^2)] - (\vec{k}_1 - \vec{k}_3)^2 + i\eta,$$

$$D_b = q_b^2 + i\eta = -M_B^2x_3(1-r^2) - \vec{k}_3^2 + i\eta,$$

$$D_{q_1} = q_{q_1}^2 + i\eta = M_B^2[x_1^2 - x_1(1-r^2)] - \vec{k}_1^2 + i\eta. \quad (3.5)$$

The approximation made here was to take  $m_b \approx M_B$  in the propagator of the heavy  $b$  quark. Other propagators are massless.

The operators  $\mathcal{O}_4(\mathcal{O}_{10})$  and  $\mathcal{O}_6(\mathcal{O}_8)$  also receive nonfactorizable contributions coming from the estimation of the diagrams in Fig. 3(b). The expressions for the  $\mathcal{O}_4(\mathcal{O}_{10})$  operator are

$$T_{nonfact}(\mathcal{O}_4) = T_C(\mathcal{O}_4) + T_D(\mathcal{O}_4),$$

$$\begin{aligned} T_C(\mathcal{O}_4) &= -4\pi\alpha_s(\mu) \frac{C_F}{3} \frac{N_c}{\sqrt{3}} \frac{1}{2\sqrt{2}} 32M_B^3 r \\ &\times [(1-r^2)(1-x_1-x_2)\epsilon \cdot p_1] \cdot \frac{1}{D_G} \frac{1}{D_{q_2}}, \\ T_D(\mathcal{O}_4) &= -4\pi\alpha_s(\mu) \frac{C_F}{3} \frac{N_c}{\sqrt{3}} \frac{1}{2\sqrt{2}} 32M_B^3 r \\ &\times [(2x_1-x_2-x_3 \\ &-r^2(x_2-x_3))\epsilon \cdot p_3] \cdot \frac{1}{D_G} \frac{1}{D_{q_3}}, \end{aligned} \quad (3.6)$$

and similarly for the  $\mathcal{O}_6(\mathcal{O}_8)$  operator

$$\begin{aligned} T_{nonfact}(\mathcal{O}_6) &= T_C(\mathcal{O}_6) + T_D(\mathcal{O}_6), \\ T_C(\mathcal{O}_6) &= -4\pi\alpha_s(\mu) \frac{C_F}{3} \frac{N_c}{\sqrt{3}} \frac{1}{2\sqrt{2}} 32M_B^3 r \\ &\times [(1-2x_1-x_2+x_3 \\ &+r^2(1-x_2-x_3))\epsilon \cdot p_3] \cdot \frac{1}{D_G} \frac{1}{D_{q_2}}, \\ T_D(\mathcal{O}_6) &= -4\pi\alpha_s(\mu) \frac{C_F}{3} \frac{N_c}{\sqrt{3}} \frac{1}{2\sqrt{2}} 32M_B^3 r \\ &\times [(1-r^2)(x_1-x_2)\epsilon \cdot p_1] \cdot \frac{1}{D_G} \frac{1}{D_{q_3}}. \end{aligned} \quad (3.7)$$

The denominators of the virtual quark propagators in Fig. 3(b) are

$$\begin{aligned} D_{q_2} &= q_{q_2}^2 + i\eta = M_B^2 [(1-x_1-x_3)(-(x_1-x_3) \\ &+ (1-x_2-x_3)r^2)] - (\vec{k}_1 + \vec{k}_2 - \vec{k}_3)^2 + i\eta, \\ D_{q_3} &= q_{q_3}^2 + i\eta = M_B^2 [(x_1-x_2)((x_1-x_3) \\ &- (x_2-x_3)r^2)] - (\vec{k}_1 - \vec{k}_2 - \vec{k}_3)^2 + i\eta. \end{aligned} \quad (3.8)$$

The calculation of the one-loop EW-penguinlike contributions from Fig. 3(c) follows the already familiar procedure. Both diagrams  $A_{loop}$  and  $B_{loop}$  are proportional to their skeleton graphs  $A$  and  $B$ , respectively. Performing renormalization consistent with the use of the NLO weak Hamiltonian and its renormalization-scheme independence [15], the result, as expected, is given by

$$-3T_{fact} \cdot \frac{\alpha_s}{9\pi} \left( \frac{10}{9} - \Delta G(m_q^2, M_\phi^2, \mu^2) \right), \quad (3.9)$$

where  $\Delta G$  has already been defined by Eq. (2.4) and the value of the parameter  $q^2$  is determined from momentum distributions in the process to be  $M_\phi^2$ .

The contributions from other two penguinlike diagrams, Fig. 3(d), are lengthy because they involve the  $b \rightarrow d \gamma^* g^*$  vertex calculation [16] and will be given only in the final form, in expression (3.17), and in the Appendix.

The next step to be performed is to express the hard scattering amplitudes, Eqs. (3.4), (3.6), (3.7) in the Fourier-transformed space of transverse momenta. The Fourier-transformed amplitudes read

$$\begin{aligned} \tilde{T}_{fact} &= -\frac{\alpha_s(\mu)}{\pi} \cdot \frac{C_F}{3} \frac{N_c}{\sqrt{3}} \frac{1}{2\sqrt{2}} 32M_B^3 r \\ &\times \{ [(1+x_3(1-r^2))\epsilon \cdot p_3] \\ &\times h_A(D_G, D_b, b_1, b_3) \\ &+ [x_1(1-r^2)\epsilon \cdot p_1 - x_1\epsilon \cdot p_3] \\ &\times h_B(D_G, D_{q_1}, b_3, b_1) \}, \\ \tilde{T}_{nonfact}(\mathcal{O}_4) &= -\frac{\alpha_s(\mu)}{\pi} \cdot \frac{C_F}{3} \frac{N_c}{\sqrt{3}} \frac{1}{2\sqrt{2}} 32M_B^3 r \\ &\times \{ [(1-r^2)(1-x_1-x_2)\epsilon \cdot p_1] \\ &\times h_C(D_{q_2}, D_G, b_2, b_1) \\ &+ [(2x_1-x_2-x_3-r^2(x_2-x_3))\epsilon \cdot p_3] \\ &\times h_D(D_{q_3}, D_G, b_2, b_1) \}, \\ \tilde{T}_{nonfact}(\mathcal{O}_6) &= -\frac{\alpha_s(\mu)}{\pi} \cdot \frac{C_F}{3} \frac{N_c}{\sqrt{3}} \frac{1}{2\sqrt{2}} 32M_B^3 r \\ &\times \{ [(1-2x_1-x_2+x_3 \\ &+ r^2(1-x_2-x_3))\epsilon \cdot p_3] \cdot h_C \\ &\times (D_{q_2}, D_G, b_2, b_1) \\ &+ [(1-r^2)(x_1-x_2)\epsilon \cdot p_1] \\ &\times h_D(D_{q_3}, D_G, b_2, b_1) \}, \end{aligned} \quad (3.10)$$

where

$$\begin{aligned} h_A(D_G, D_b, b_1, b_3) &= K_0(\sqrt{-q_G^2}|\vec{b}_1|) \\ &\times K_0(\sqrt{-q_b^2}|\vec{b}_1 + \vec{b}_3|) \delta(\vec{b}_2), \\ h_B(D_G, D_{q_1}, b_3, b_1) &= K_0(\sqrt{-q_G^2}|\vec{b}_3|) \\ &\times K_0(\sqrt{-q_{q_1}^2}|\vec{b}_1 + \vec{b}_3|) \delta(\vec{b}_2), \\ h_C(D_{q_2}, D_G, b_2, b_1) &= K_0(\sqrt{-q_{q_2}^2}|\vec{b}_2|) \\ &\times K_0(\sqrt{-q_G^2}|\vec{b}_1 - \vec{b}_2|) \delta(\vec{b}_1 + \vec{b}_3), \\ h_D(D_{q_3}, D_G, b_2, b_1) &= K_0(\sqrt{-q_{q_3}^2}|\vec{b}_2|) \\ &\times K_0(\sqrt{-q_G^2}|\vec{b}_1 - \vec{b}_2|) \delta(\vec{b}_1 + \vec{b}_3), \end{aligned} \quad (3.11)$$

and  $K_0$  is the modified Bessel function of order zero.

For the scales  $\mu$  appearing in formulas (3.10) and (3.9) we are going to take the largest mass scale in the particular diagram:

$$\begin{aligned} t_A &= \max(\sqrt{-q_G^2}, \sqrt{-q_b^2}, 1/b_1, 1/b_3), \\ t_B &= \max(\sqrt{-q_G^2}, \sqrt{-q_{q_1}^2}, 1/b_1, 1/b_3), \\ t_C &= \max(\sqrt{-q_G^2}, \sqrt{-q_{q_2}^2}, 1/b_1, 1/b_2), \\ t_D &= \max(\sqrt{-q_G^2}, \sqrt{-q_{q_3}^2}, 1/b_1, 1/b_2), \\ t_{loop} &= \max(\sqrt{-q_G^2}, 1/b_1), \end{aligned} \quad (3.12)$$

which ensures the reliable perturbative calculations with the small  $\alpha_s$  coupling.

Performing trivial  $b$  integrations over  $\delta$  functions and performing angular integrations by using Graph's theorem:

$$\begin{aligned} f(x, b_1, b_2) &= \int d\phi K_0(x|\vec{b}_1 \pm \vec{b}_2|) \\ &= 2\pi[\Theta(b_1 - b_2)K_0(xb_1)I_0(xb_2) \\ &\quad + \Theta(b_2 - b_1)K_0(xb_2)I_0(xb_1)], \end{aligned} \quad (3.13)$$

one can finally write the total amplitude of the  $B^- \rightarrow \pi^- \phi$  decay as

---


$$\begin{aligned} \mathcal{M} &= \langle \pi \phi | H_{eff} | B \rangle = \frac{G_F}{\sqrt{2}} \sum_{q=u,c} V_q \mathcal{A}_q, \\ \mathcal{A}_q &= \left\{ 3 \left( \bar{c}_3 + \bar{c}_5 - \frac{1}{2}(\bar{c}_7 + \bar{c}_9) \right) + \bar{c}_4 + \bar{c}_6 - \frac{1}{2}(\bar{c}_8 + \bar{c}_{10}) \right\} \langle T_{fact} \rangle + \left( \bar{c}_4 - \frac{1}{2}\bar{c}_{10} \right) \langle T_{nonfact}(\mathcal{O}_4) \rangle + \left( \bar{c}_6 - \frac{1}{2}\bar{c}_8 \right) \langle T_{nonfact}(\mathcal{O}_6) \rangle \\ &\quad - \frac{\alpha_{em}}{9\pi} (3\bar{c}_1 + \bar{c}_2) \cdot 3 \langle T_{fact} \rangle \left( \frac{10}{9} - \Delta G(m_q^2, M_\phi^2, m_b^2) \right) - \frac{2\alpha_{em}}{3\pi} \bar{c}_2 \langle T_{loop} \rangle_q, \end{aligned} \quad (3.14)$$

with the matrix elements

$$\begin{aligned} \langle T_{fact} \rangle &= -\frac{C_F}{3} f_\phi M_B^3 r \int dx_1 dx_3 \int b_1 db_1 b_3 db_3 \Phi_B(x_1, b_1) \Phi_\pi^*(x_3, b_3) \times \left\{ \frac{\alpha_s(t_A)}{\pi} H(D_G, D_b, b_1, b_3) \right. \\ &\quad \times [(1 + x_3(1 - r^2)) \epsilon \cdot p_3] e^{-(S_B(t_A) + S_\pi(t_A))} + \frac{\alpha_s(t_B)}{\pi} H(D_G, D_{q_1}, b_3, b_1) \\ &\quad \times [x_1(1 - r^2) \epsilon \cdot p_1 - x_1 \epsilon \cdot p_3] e^{-(S_B(t_B) + S_\pi(t_B))} \Big\}, \\ \langle T_{nonfact}(\mathcal{O}_4) \rangle &= -\frac{C_F}{3} f_\phi M_B^3 r \int [dx] \int b_1 db_1 b_2 db_2 \Phi_B(x_1, b_1) \frac{\tilde{\Phi}_\phi^*(x_2, b_2)}{4\pi} \Phi_\pi^*(x_3, b_1) \\ &\quad \times \left\{ \frac{\alpha_s(t_C)}{\pi} H(D_{q_2}, D_b, b_2, b_1) [(1 - r^2)(1 - x_1 - x_2) \epsilon \cdot p_1] e^{-(S_B(t_C) + S_\phi(t_C) + S_\pi(t_C))|_{b_3=b_1}} \right. \\ &\quad \left. + \frac{\alpha_s(t_D)}{\pi} H(D_{q_3}, D_b, b_2, b_1) [(2x_1 - x_2 - x_3 - r^2(x_2 - x_3)) \epsilon \cdot p_3] \times e^{-(S_B(t_D) + S_\phi(t_D) + S_\pi(t_D))|_{b_3=b_1}} \right\}, \\ \langle T_{nonfact}(\mathcal{O}_6) \rangle &= -\frac{C_F}{3} f_\phi M_B^3 r \int [dx] \int b_1 db_1 b_2 db_2 \Phi_B(x_1, b_1) \frac{\tilde{\Phi}_\phi^*(x_2, b_2)}{4\pi} \Phi_\pi^*(x_3, b_1) \\ &\quad \times \left\{ \frac{\alpha_s(t_C)}{\pi} H(D_{q_2}, D_b, b_2, b_1) [(1 - 2x_1 - x_2 + x_3 + r^2(1 - x_2 - x_3)) \epsilon \cdot p_3] e^{-(S_B(t_C) + S_\phi(t_C) + S_\pi(t_C))|_{b_3=b_1}} \right. \\ &\quad \left. + \frac{\alpha_s(t_D)}{\pi} H(D_{q_3}, D_b, b_2, b_1) [(1 - r^2)(x_1 - x_2) \epsilon \cdot p_1] e^{-(S_B(t_D) + S_\phi(t_D) + S_\pi(t_D))|_{b_3=b_1}} \right\}, \end{aligned} \quad (3.15)$$

where the Fourier-transformed expressions for the propagators in Eqs. (3.15) have the general form

$$H(D_1, D_2, b_1, b_2) = K_0(\sqrt{-D_1}b_1)f(\sqrt{-D_2}, b_1, b_2), \quad (3.16)$$

with the function  $f$  as defined by (3.13).

In Eq. (3.14) we have also included the one-loop contributions from the diagrams of Figs. 3(c) and 3(d). The matrix elements receiving the contributions from the diagrams in Fig. 3(d) are

$$\begin{aligned} \langle T_{loop} \rangle_q = & -\frac{C_F}{3} f_\phi M_B^3 r \int dx_1 dx_3 \int b_1 db_1 \Phi_B(x_1, b_1) \\ & \times \Phi_\pi^*(x_3, b_1) \frac{1}{M_\phi^2} \left\{ \frac{\alpha_s(t_{loop})}{\pi} K_0(\sqrt{-q_G^2} b_1) \right. \\ & \left. \times [T_q^E + T_q^F] e^{-(S_B(t_{loop}) + S_\pi(t_{loop}))|_{b_3=b_1}} \right\}. \quad (3.17) \end{aligned}$$

The expressions for  $T_q^E$  and  $T_q^F$  are given explicitly in the Appendix.

One should note that in the above expressions we have pulled out the normalization factor  $f_\phi/2\sqrt{6}$  ( $f_\phi$  is the  $\phi$ -meson decay constant) of the  $\phi$  wave function and we denote the rest by  $\tilde{\Phi}_\phi$  in order to have the same prefactor in both factorizable and nonfactorizable contributions.

From the expression for  $\langle T_{fact} \rangle$  in Eq. (3.15) it is easy to essentially recognize the factorization structure in which a matrix element of a four-quark operator factorizes in the product of two current matrix elements  $\langle \phi | (\bar{s}s)_{V-A} | 0 \rangle \cdot \langle \pi^-(p_3) | (\bar{d}b)_{V-A} | B^-(p_1) \rangle \sim f_\phi \epsilon^{\mu\nu} \cdot (Ap_1^\mu + Bp_3^\mu)$ , and the  $\phi$ -meson wave function integrates out. The current matrix element  $\langle \pi^-(p_3) | (\bar{d}b)_{V-A} | B^-(p_1) \rangle$  exactly describes the  $B \rightarrow \pi$  transition form factor at the momentum transfer  $p^2 = (p_1 - p_3)^2 = M_\phi^2$ . In Sec. IV we use this form factor to select mesonic wave functions.

The expressions for the Sudakov exponents  $S_\pi$ ,  $S_\phi$ , and  $S_B$  in Eqs. (3.15) and (3.17) are given in Sec. IV.

#### IV. MESONIC WAVE FUNCTIONS AND SUDAKOV FACTORS

The calculation of the matrix elements requires the knowledge of the scalar meson wave functions  $\Phi$ . The hadronic wave functions represent the most speculative part of the perturbative approach. They are of nonperturbative origin and should be a universal, process-independent quantity.

However, even for the most theoretically and experimentally exploited hadron, namely, the pion there are contradictory conclusions about the specific form of  $\Phi_\pi$ . Theoretical calculations performed by using the QCD sum-rule method [17] and on the lattice [18] cannot distinguish between the most promising forms of the pion wave function, the asymptotic one

$$\Phi_\pi^{as}(x) = 6x(1-x) \frac{f_\pi}{2\sqrt{6}}, \quad (4.1)$$

and the Chernyak-Zhitnitsky (CZ) wave function [17]

$$\Phi_\pi^{CZ}(x) = 30x(1-x)(1-2x)^2 \frac{f_\pi}{2\sqrt{6}}, \quad (4.2)$$

both normalized to satisfy the experimentally obtained value for the pion decay constant  $f_\pi = 0.133$  GeV. In addition, any comparison between theoretically calculable processes and existing experiments cannot provide an unambiguous determination between them [19].

What we are going to regard as the CZ wave function throughout the paper is the CZ form in which the evolution from the hadronic scale  $\mu_0 \sim 0.5$  GeV to some scale  $\mu_1$  is included [20]:

$$\begin{aligned} \Phi_\pi^{CZ}(x, \mu_1) = & 6x(1-x) \left[ 1 + (5(1-2x)^2 - 1) \right. \\ & \left. \times \left( \frac{\alpha_s(\mu_1)}{\alpha_s(\mu_0)} \right)^{50/81} \right] \frac{f_\pi}{2\sqrt{6}}, \quad (4.3) \end{aligned}$$

and, in the modified perturbative approach, the scale  $\mu_1$  is taken to be  $1/b$  [21].

If we are going to retain the intrinsic  $b$  dependence of the wave functions  $\Phi$  in the expressions for the matrix elements, then we are faced with even more uncertainties coming from the ambiguity in the form of the wave function  $b$ -part as well as in the values of some new parameters.

The constituent quark model of the wave function associates some Gaussian exponential to the  $b$ -dependent part [22], so that

$$\Phi_\pi^{as}(x, b) = 6x(1-x) 4\pi \exp(-x(1-x)b^2/(4a_{as}^2)) \frac{f_\pi}{2\sqrt{6}} \quad (4.4)$$

and

$$\begin{aligned} \Phi_\pi^{CZ}(x, b, \mu_1) = & 6x(1-x) \\ & \times \left[ 1 + (5(1-2x)^2 - 1) \left( \frac{\alpha_s(\mu_1)}{\alpha_s(\mu_0)} \right)^{50/81} \right] \\ & \times 4\pi \exp(-x(1-x)b^2/(4a_{CZ}^2)) \frac{f_\pi}{2\sqrt{6}}, \quad (4.5) \end{aligned}$$

where the pion's transverse parameters  $a_{as}$  and  $a_{CZ}$  are fixed from the  $\pi \rightarrow \gamma\gamma$  process to be  $a_{as} = 0.846$  GeV<sup>-1</sup> and  $a_{CZ} = 0.655$  GeV<sup>-1</sup>, respectively [23].

For a  $B$ -meson wave function there exist a few models [24]. We consider two forms that have been proved in the calculations of various nonleptonic  $B$  decays. The first one is [25]



$$\Phi_B^{(1)}(x, \vec{k}) = N^{(1)} \left[ C + \frac{m_b^2}{1-x} + \frac{\vec{k}^2}{x(1-x)} \right]^{-2}, \quad (4.6)$$

whose Fourier transform gives

$$\begin{aligned} \Phi_B^{(1)}(x, b) &= \frac{N^{(1)}}{4\pi} \frac{bx^2(1-x)^2}{\sqrt{M_B^2 x + Cx(1-x)}} \\ &\times K_1(\sqrt{M_B^2 x + Cx(1-x)}b), \end{aligned} \quad (4.7)$$

with the approximation  $m_b \simeq M_B = 5.28$  GeV.  $K_1$  is the modified Bessel function of order one. Neglecting the  $b$  dependence leads to

$$\Phi_B^{(1)}(x) = \frac{N^{(1)}}{16\pi^2} \frac{x(1-x)^2}{M_B^2 + C(1-x)}. \quad (4.8)$$

For the constants  $N^{(1)}$  and  $C$  we have used the fitted parameters  $N^{(1)} = 604.34$  GeV<sup>3</sup> and  $C = -27.5$  GeV<sup>2</sup>, which have been proved in other calculations [26].

Another model is the oscillatorlike wave function of Bauer, Stech, and Wirbel [27]:

$$\Phi_B^{(2)}(x, b) = \frac{N^{(2)}}{2\pi} \sqrt{x(1-x)} \exp\left(-\frac{M_B^2}{2\omega^2} x^2\right) \exp\left(-\frac{\omega^2}{2} b^2\right), \quad (4.9)$$

with the constants  $N^{(2)} = 156.34$  GeV and  $\omega = 0.4$  GeV. Both wave functions, Eqs. (4.7) and (4.9), are normalized with  $f_B = 200$  MeV.

The vector-meson wave functions are modeled in the QCD sum-rule calculations [17,28]. Since the form of the  $\phi$ -meson wave function is still questionable, we have decided to use the asymptotic form

$$\Phi_\phi(x) = 6x(1-x) \frac{f_\phi}{2\sqrt{6}}, \quad f_\phi = 0.233 \text{ GeV}, \quad (4.10)$$

without including any  $b$  dependence. We believe that owing to the lack of better experimental data to which transverse parameters can be fixed, an unrealistic  $b$ -dependent part may produce more questionable results than by neglecting it.

In order to suppress the soft contributions in the hard scattering amplitudes (3.15), (3.17), we have included the Sudakov factors [13]. They ensure that the hard scattering amplitude receives contributions only from the exchange of hard gluons, suppressing the contributions of soft gluons from the large  $b$  region. The Sudakov suppression is comprised by the hadron wave function redefinition

$$\begin{aligned} \Phi_B &\rightarrow \Phi_B(x_1, b_1) \exp(-S_B(t)), \\ \Phi_\phi &\rightarrow \Phi_\phi(x_2, b_2) \exp(-S_\phi(t)), \\ \Phi_\pi &\rightarrow \Phi_\pi(x_3, b_3) \exp(-S_\pi(t)). \end{aligned} \quad (4.11)$$

The Sudakov exponentials exhibit the result of all-order resummation of double logs appearing from the overlap of collinear and soft divergences [29]. In our case,

$$\begin{aligned} S_B(t) &= s(x_1 p_1^-, b_1, t) - 1/\beta_0 \ln\left(\frac{\ln(t/\Lambda_{QCD})}{\ln(1/(b_1 \Lambda_{QCD}))}\right), \\ S_\phi(t) &= s(x_2 p_2^+, b_2, t) + s(((1-x_2)p_2^+), b_2, t) \\ &\quad - 1/\beta_0 \ln\left(\frac{\ln(t/\Lambda_{QCD})}{\ln(1/(b_2 \Lambda_{QCD}))}\right), \\ S_\pi(t) &= s(x_3 p_3^-, b_3, t) + s(((1-x_3)p_3^-), b_3, t) \\ &\quad - 1/\beta_0 \ln\left(\frac{\ln(t/\Lambda_{QCD})}{\ln(1/(b_3 \Lambda_{QCD}))}\right), \end{aligned} \quad (4.12)$$

where  $\beta_0 = (33 - 2n_f)/12$  and  $n_f = 4$ . For  $\Lambda_{QCD}$  we have used the value  $\Lambda_{QCD} = 0.2$  GeV throughout the paper. The last term in the above expressions accounts for the renormalization from the IR scale  $1/b$  to the some renormalization scale  $t$ , which we are going to take to be one of the scales from Eq. (3.12), depending on the diagram considered.

The full expressions for the Sudakov functions  $s(x_i, b_i, t)$ , together with the usual approximations used in a numerical treatment, can be found in [30].

Note that we have also associated the Sudakov function  $s(x_1 p_1^-, b_1, t)$  with the light antiquark of the  $B$  meson. The heavy  $b$  quark, having a finite mass, does not produce collinear divergences and its Sudakov function is zero.

Use of the above mentioned diversity of the wave functions would certainly diminish the capability of perturbative calculations for giving reliable predictions for the  $B^- \rightarrow \pi^- \phi$  branching ratio and  $CP$  asymmetry, having in mind that the effects of the large reduction of the results owing to the intrinsic  $b$  dependence in the wave functions as well as the large difference in the predictions depending on the  $B$  and  $\pi$  meson wave function employed, has already been observed in other perturbative calculations [31]. We have checked that this is also the case in the calculation of the  $B \rightarrow \pi \phi$  decay.

Owing to the specific character of the  $B \rightarrow \pi \phi$  decay governed by the  $b \rightarrow d s \bar{s}$  transition where the strange quark-antiquark pair has to form the final  $\phi$ -meson state, we can assume that the  $B \rightarrow \pi \phi$  process is determined predominantly by the  $B \rightarrow \pi$  transition at the energy  $p^2 = M_\phi^2$ .

Therefore, we can try to make a selection among the wave functions by comparing the results for the  $B \rightarrow \pi$  transition form factor obtained from the QCD sum rule [32] and lattice calculations [33] summarized in

$$F_+^{B \rightarrow \pi}(0) = 0.25 - 0.35, \quad (4.13)$$

with those estimated in our modified perturbative approach.

The expression for the form factor in the perturbative approach has the form

$$\begin{aligned}
F_{+}^{B \rightarrow \pi}(\eta) = & \frac{C_F}{2} M_B^2 \int dx_1 dx_3 \int b_1 db_1 b_3 db_3 \Phi_B(x_1, b_1) \\
& \times \Phi_{\pi}^*(x_3, b_3) \left\{ \frac{\alpha_s(t_A)}{\pi} H(D_G, D_b, b_1, b_3) \right. \\
& \times [1 + x_3 \eta] e^{-(S_B(t_A) + S_{\pi}(t_A))} \\
& + \frac{\alpha_s(t_B)}{\pi} H(D_G, D_{q_1}, b_3, b_1) \\
& \left. \times [-x_1(1 - \eta)] e^{-(S_B(t_B) + S_{\pi}(t_B))} \right\}, \quad (4.14)
\end{aligned}$$

which can be easily recognized in the expression for the factorizable part of the  $B \rightarrow \pi \phi$  decay, Eq. (3.15). The parameter  $\eta$  is the fraction of the energy of the  $\pi$  meson and at the momentum transfer  $p^2 = 0$  or  $p^2 = M_{\phi}^2$  we have  $\eta = 1$  or  $\eta = 1 - M_{\phi}^2/M_B^2 = 1 - r^2$ , respectively.

Estimating the  $B \rightarrow \pi$  transition form factor at the momentum transfer  $p^2 = 0$  using different forms of the  $B$  and  $\pi$  meson wave functions taken from above, we achieve predictions which are far from the values obtained in the QCD sum rule and lattice calculations (4.13), except if we assume the oscillatorlike model for the  $B$  meson wave function  $\Phi_B^{(2)}(x)$ , Eq. (4.9), and the CZ type of the pion wave function (4.3), both being intrinsic  $b$  independent. Our predicted value for the  $B \rightarrow \pi$  form factor obtained with these wave functions is

$$F_{pert}^{B \rightarrow \pi}(0) = 0.282. \quad (4.15)$$

Both,  $\Phi_B^{(2)}(x)$  and  $\Phi_{\pi}^{CZ}(x, \mu_1)$  are more end-point concentrated wave functions than their alternative forms,  $\Phi_B^{(1)}(x)$  (4.8) and  $\Phi_{\pi}^{as}(x)$  (4.1), respectively. This indicates a need for the enhancement of the soft contributions in order to match the predictions (4.13) for the  $B \rightarrow \pi$  form factor estimated by nonperturbative methods.

Comparable calculations of the  $B \rightarrow \pi$  form factor in the modified perturbative approach have also been performed in [22,31] and, similarly, the results obtained have exhibited strong dependence on the mesonic wave functions used, confirming that the wave functions represent the weakest point in the calculation of  $B$ -meson decays in the perturbative approach.

## V. NUMERICAL RESULTS AND DISCUSSIONS

Now we are going to discuss the branching ratio  $BR$  and the  $CP$  asymmetry in the  $B^- \rightarrow \pi^- \phi$  decay numerically.

The decay rate is given as

$$\Gamma(B^- \rightarrow \pi^- \phi) = \frac{1}{16\pi} \frac{\lambda^{1/2}(M_B, M_{\phi}, 0)}{M_B^3} |\mathcal{M}|^2, \quad (5.1)$$

where  $\lambda^{1/2}(M_B, M_{\phi}, 0) = M_B^2(1 - r^2)$  and the total amplitude  $\mathcal{M}$  is given by Eq. (3.14).  $CP$  asymmetry in terms of the  $\mathcal{A}_u$  and  $\mathcal{A}_c$  amplitudes, Eq. (3.14), reads

$$a_{CP} = \frac{-2V_c \text{Im}(V_u) \text{Im}(\mathcal{A}_u \mathcal{A}_c^*)}{(|V_u|^2 |\mathcal{A}_u|^2 + |V_c|^2 |\mathcal{A}_c|^2 + 2V_c \text{Re}(V_u) \text{Re}(\mathcal{A}_u \mathcal{A}_c^*))}. \quad (5.2)$$

The products of the CKM matrix elements may be written in the Wolfenstein parametrization as

$$\begin{aligned}
V_u &= V_{ud}^* V_{ub} = A\lambda^3(1 - \lambda^2/2)(\rho - i\eta) \equiv A\lambda^3(\bar{\rho} - i\bar{\eta}), \\
V_c &= V_{cd}^* V_{cb} = -A\lambda^3. \quad (5.3)
\end{aligned}$$

We use the following values of the parameters  $\bar{\rho}$  and  $\bar{\eta}$ :

$$\bar{\rho} = 0.16, \quad \bar{\eta} = 0.33, \quad (5.4)$$

which correspond to their central values obtained by the unitarity fit [34]. Since recent measurements disfavor the negative values for the  $\rho$  parameter [35], the  $CP$  asymmetries will be presented in figures by taking  $\bar{\rho}$  in the range

$$0 \leq \bar{\rho} \leq 0.25 \quad (5.5)$$

and using the central value for the  $\bar{\eta}$  parameter from Eq. (5.4), the minimum and the maximum allowed values [34]

$$\begin{aligned}
\bar{\eta} &= 0.27, \\
\bar{\eta} &= 0.38, \quad (5.6)
\end{aligned}$$

respectively. The other Wolfenstein CKM parameters used are  $A = 0.823$  and  $\lambda = 0.2196$ .

Following Ref. [36], we are going to take the constituent quark masses in the loop expressions, Eqs. (2.4) and (3.17), with particular values  $m_u = 0.2$  GeV and  $m_c = 1.5$  GeV.

For the Wilson scale-independent coefficients at the renormalization scale  $\mu = m_b = 4.8$  GeV [ $\alpha_s(M_Z) = 0.118$ ,  $\alpha_{em}(M_Z) = 1/128$ ] we take [37]

$$\begin{aligned}
\bar{c}_1 &= -0.324, \quad \bar{c}_2 = 1.15, \\
\bar{c}_3 &= 0.017, \quad \bar{c}_4 = -0.038, \\
\bar{c}_5 &= 0.011, \quad \bar{c}_6 = -0.047, \\
\bar{c}_7 &= -1.05 \times 10^{-5}, \quad \bar{c}_8 = -3.84 \times 10^{-4}, \\
\bar{c}_9 &= -0.0101, \quad \bar{c}_{10} = 1.96 \times 10^{-3}. \quad (5.7)
\end{aligned}$$

One can note from expression (5.2) that some absorptive part in the amplitude is essential for nonvanishing  $CP$  asymmetry.

As in the BSW factorization approach, the necessary absorptive part comes from the cut in the penguinlike diagrams in Fig. 3(c), residing in the term  $\Delta G(m_q^2, M_{\phi}^2, \mu^2)$ . From expression (2.4) it is easy to see that the absorptive part is developed for the virtual photon momentum  $q$  such that  $q^2 \geq 4m_q^2$ ,  $q = u, c$ . Owing to the specific momentum distributions in the  $B^- \rightarrow \pi^- \phi$  process, the imaginary part emerges

only from the diagram with a  $u$  quark in the loop. In numerical calculations we use the approximation of Eq. (2.4),

$$\Delta G_{app}(m_q^2, M_\phi^2, \mu^2) = \frac{2}{3} \left[ \frac{5}{3} + \frac{4}{z} + \left( 1 + \frac{2}{z} \right) R(z) - \ln \frac{m_q^2}{\mu^2} \right], \quad (5.8)$$

where by defining  $a = \sqrt{|1 - 4/z|}$ , we have

$$R(z) = \begin{cases} -a\pi + 2a \arctan(a), & z = (M_\phi/m_c)^2, \\ ia\pi + a \ln \frac{1-a}{1+a}, & z = (M_\phi/m_u)^2. \end{cases} \quad (5.9)$$

In addition, in the perturbative approach there are absorptive parts connected with the cuts in the propagators of virtual partons in each of the diagrams in Fig. 3. The expression for  $H$ , Eq. (3.16), can develop the imaginary part for some of the values of the fractions  $x_i$  in the integration for which the denominators of the gluon or quark propagators under the square root become negative [see Eqs. (3.5), (3.8)]. In this case we take

$$K_0(iyb) = \frac{i\pi}{2} H_0^{(1)}(yb) \quad (5.10)$$

and

$$f(iy, b_1, b_2) = \frac{i\pi}{2} [\Theta(b_1 - b_2) H_0^{(1)}(yb_1) J_0(yb_2) + \Theta(b_2 - b_1) H_0^{(1)}(yb_2) J_0(yb_1)]. \quad (5.11)$$

Having selected the B meson wave function  $\Phi_B^{(2)}(x)$ , Eq. (4.9), in the preceding section:

$$\Phi_B^{(2)}(x) = \frac{1}{4\pi} \Phi_B^{(2)}(x, 0) = \frac{N^{(2)}}{8\pi^2} \sqrt{x(1-x)} \exp\left(-\frac{M_B^2}{2\omega^2} x^2\right), \quad (5.12)$$

and the  $\Phi_\pi^{CZ}(x, 1/b)$  Eq. (4.3) for the  $\pi$  meson wave function, we can now continue along the lines developed in the preceding sections and give reliable predictions for the  $B^- \rightarrow \pi^- \phi$  branching ratio and  $CP$  asymmetry in the modified perturbative approach, using the NLO weak Hamiltonian.

The results are presented in Tables I and II, together with the predictions estimated in the BSW factorization approach, both being calculated with the preferred values of the CKM parameters,  $\bar{\rho} = 0.16$  and  $\bar{\eta} = 0.33$ .

Calculations of the  $B^- \rightarrow \pi^- \phi$  branching ratio and asymmetry in the BSW factorization approach have been performed by many authors [3–6]. In order to be able to clearly assign the role of nonfactorizable contributions in the decay, we have recalculated the BSW factorization predictions using our values of the Wilson coefficients  $\bar{c}_i$  (5.7) and the CKM parameters  $\bar{\rho}$  and  $\bar{\eta}$ .

The decay amplitude in the BSW approach can be directly compared with the complete expression for the  $B \rightarrow \pi \phi$  am-

TABLE I. Branching ratios for the  $B^- \rightarrow \pi^- \phi$  decay calculated for different penguin contributions, by taking only the factorizable parts or the complete expression into account. The first column contains the predictions obtained in the BSW factorization approach by using  $\langle q^2 \rangle = M_\phi^2$  (see text). Columns I and II give predictions calculated in the modified perturbative approach by employing the meson wave functions  $\Phi_B^{(2)}(x)$ , Eq. (5.12) and  $\Phi_\pi^{CZ}(x, 1/b)$ , Eq. (4.3), and by using the Wilson coefficients  $\bar{c}_k(m_b)$  (5.7) in column I and  $\bar{c}_k^{(0)}(t)$  (5.16) in column II. The CKM parameters used are  $\bar{\rho} = 0.16$  and  $\bar{\eta} = 0.33$ .

Penguin contributions	BR		
	BSW	I	II
QCD-factorizable	$0.20 \times 10^{-10}$	$0.14 \times 10^{-10}$	$1.06 \times 10^{-10}$
QCD-all		$2.51 \times 10^{-10}$	$0.73 \times 10^{-10}$
QCD+QED-factorizable	$0.34 \times 10^{-8}$	$0.38 \times 10^{-8}$	$0.89 \times 10^{-8}$
QCD+QED-all		$0.44 \times 10^{-8}$	$0.85 \times 10^{-8}$

plitude given by Eq. (3.14) by neglecting nonfactorizable parts and numerically suppressed contributions emerging from the diagrams in Fig. 3(d). The matrix element in the strict factorization approach is proportional to the  $F^{B \rightarrow \pi}(M_\phi^2)$  form factor which we calculate in the single-pole approximation as

$$F_{BSW}^{B \rightarrow \pi}(M_\phi^2) = \frac{F_{BSW}^{B \rightarrow \pi}(0)}{1 - M_\phi^2/M_{B\pi}^2(1^-)}, \quad (5.13)$$

where  $M_{B\pi}^2(1^-) = 5.32 \text{ GeV}^2$  and  $F_{BSW}^{B \rightarrow \pi}(0) = 0.33$  [7]. It is worth mentioning that the prediction for the  $B \rightarrow \pi$  form factor estimated in the perturbative approach, Eq. (4.15), is somewhat smaller than the  $F_{BSW}^{B \rightarrow \pi}(0)$  value.

All results estimated in the factorization approach are obtained by taking the virtual photon momentum squared equal to  $q^2 = M_\phi^2$ . We have already stated that, in general, information about the  $q^2$  value is lost by factorizing hadronic matrix elements, except in the strict factorization, when non-

TABLE II.  $CP$  asymmetries for the  $B^- \rightarrow \pi^- \phi$  decay calculated for the QCD and QED penguin contributions together, by taking only the factorizable parts or the complete expression into account. The first column contains the predictions obtained in the BSW factorization approach by using  $\langle q^2 \rangle = M_\phi^2$  (see text). Columns I and II give predictions calculated in the modified perturbative approach by employing the meson wave functions  $\Phi_B^{(2)}(x)$ , Eq. (5.12) and  $\Phi_\pi^{CZ}(x, 1/b)$ , Eq. (4.3), and by using the Wilson coefficients  $\bar{c}_k(m_b)$  (5.7) in column I and  $\bar{c}_k^{(0)}(t)$  (5.16) in column II. The CKM parameters used are  $\bar{\rho} = 0.16$  and  $\bar{\eta} = 0.33$ .

Penguin contributions	$a_{CP}/10^{-2}$		
	BSW	I	II
QCD+QED-factor of two factorizable	-1.9	14.6	15.4
QCD+QED-all		16.1	16.3

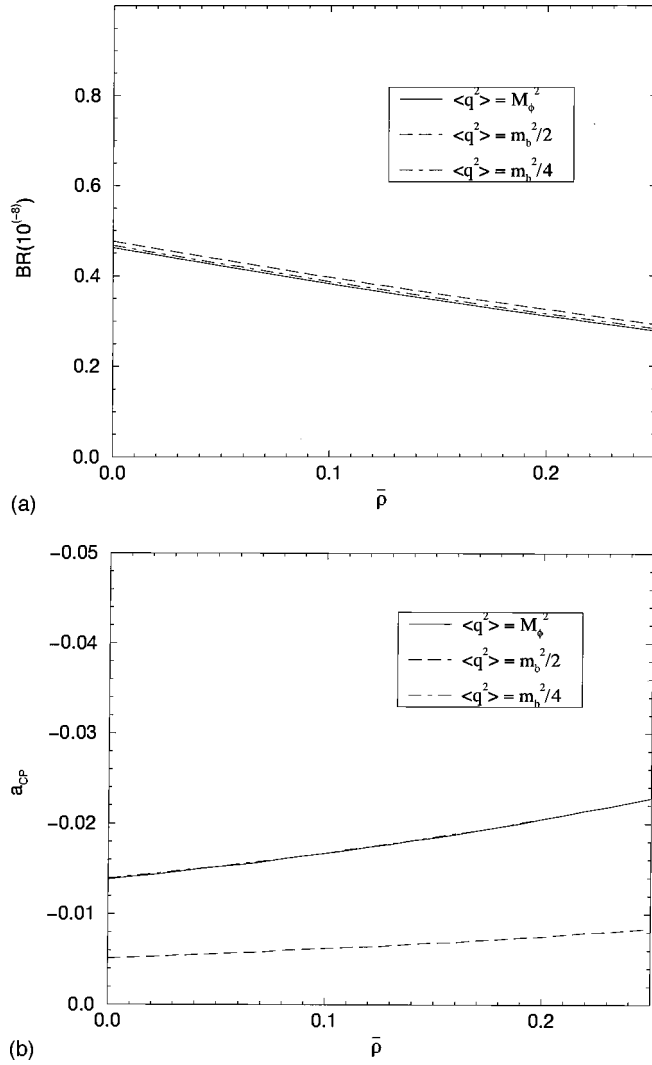


FIG. 4. Branching ratio and  $CP$  asymmetry in the  $B^- \rightarrow \pi^- \phi$  decay calculated in the BSW factorization approach as a function of the CKM parameter  $\bar{\rho}$  and for the central value of  $\bar{\eta} = 0.33$ . The solid, long dashed, and dot-dashed lines denote predictions obtained by taking  $\langle q^2 \rangle = M_\phi^2$ ,  $\langle q^2 \rangle = m_b^2/2$ , and  $\langle q^2 \rangle = m_b^2/4$ , respectively (see text).

factorizable and/or strong final-state interactions are neglected. Therefore, considering possible nonfactorizable or final-state corrections, after the factorization procedure, the  $q^2$  is usually considered as a free parameter, whose average value is constrained by some simple, general kinematical reasons to be [38]

$$m_b^2/4 \leq \langle q^2 \rangle \leq m_b^2/2, \quad (5.14)$$

and usually assumed to be valid for all nonleptonic heavy-to-light transitions.

The dependence of the branching ratio and  $CP$  asymmetry on the  $\langle q^2 \rangle$  as a function of the  $\bar{\rho}$  CKM-parameter is shown in Fig. 4. The branching ratio appears to be practically independent of the value of the  $\langle q^2 \rangle$ . Such behavior is due to the cancellation which occurs between the Wilson

coefficients multiplying the one-loop QED penguinlike matrix element, Eq. (3.14), because of the relation

$$3\bar{c}_1(m_b) \approx -\bar{c}_2(m_b). \quad (5.15)$$

On the contrary,  $CP$  asymmetry exhibits a large reduction of up to 70% if higher  $\langle q^2 \rangle$ -values are taken.

The results in column II in Tables I and II are obtained by calculation inspired by the papers of Li and collaborators [26,39], in which the  $\mu$  scale-setting ambiguity of Wilson coefficients is moderated by applying the three-scale factorization theorem. Their theorem keeps trace of all three scales characterizing the nonleptonic weak decay, the  $W$ -boson mass  $M_W$ , the typical scale  $t$  of the process, and the hadronic scale  $\sim \Lambda_{QCD}$ , and proves for the leading-order weak Hamiltonian that Wilson coefficients should be taken at the scale  $t$ , a typical scale in a particular decay. The matrix elements of the operators  $\mathcal{O}_k$  and Wilson coefficients are then both calculated at the same scale. The scale is determined by the dynamics of the process, contrary to the arbitrary renormalization scale  $\mu$  taken to be a constant,  $m_b$ , for the  $\bar{c}_k$  coefficients, Eq. (5.7).

Under the assumption that the three-scale factorization theorem is also valid for the NLO weak Hamiltonian (2.1) we have taken the explicit form of the Wilson coefficients, calculated directly at  $M_W$  and then rescaled to some lower scale  $t$  [3]:

$$\bar{c}_1^{(0)}(t) = \mathcal{O}(\alpha_s(t)) + \mathcal{O}(\alpha_{em}),$$

$$\bar{c}_2^{(0)}(t) = 1 + \mathcal{O}(\alpha_s(t)) + \mathcal{O}(\alpha_{em}),$$

$$\begin{aligned} \bar{c}_3^{(0)}(t) = & -\frac{\alpha_s(t)}{24\pi} \left[ E_0(x_t) + \frac{2}{3} \log \frac{t^2}{M_W^2} - \frac{10}{9} \right] \\ & + \frac{\alpha_{em}}{6\pi} \frac{1}{\sin^2 \Theta_W} [2B_0(x_t) + C_0(x_t)], \end{aligned}$$

$$\bar{c}_4^{(0)}(t) = \frac{\alpha_s(t)}{8\pi} \left[ E_0(x_t) + \frac{2}{3} \log \frac{t^2}{M_W^2} - \frac{10}{9} \right],$$

$$\bar{c}_5^{(0)}(t) = -\frac{\alpha_s(t)}{24\pi} \left[ E_0(x_t) + \frac{2}{3} \log \frac{t^2}{M_W^2} - \frac{10}{9} \right],$$

$$\bar{c}_6^{(0)}(t) = \frac{\alpha_s(t)}{8\pi} \left[ E_0(x_t) + \frac{2}{3} \log \frac{t^2}{M_W^2} - \frac{10}{9} \right],$$

$$\bar{c}_7^{(0)}(t) = \frac{\alpha_{em}}{6\pi} \left[ 4C_0(x_t) + D_0(x_t) + \frac{4}{9} \log \frac{t^2}{M_W^2} - \frac{20}{27} \right],$$

$$\bar{c}_8^{(0)}(t) = 0,$$

$$\begin{aligned}\bar{c}_9^{(0)}(t) &= \frac{\alpha_{\text{em}}}{6\pi} \left[ 4C_0(x_t) + D_0(x_t) + \frac{4}{9} \log \frac{t^2}{M_W^2} - \frac{20}{27} \right] \\ &\quad + \frac{\alpha_{\text{em}}}{3\pi} \frac{1}{\sin^2 \Theta_W} [5B_0(x_t) - 2C_0(x_t)], \\ \bar{c}_{10}^{(0)}(t) &= 0,\end{aligned}\tag{5.16}$$

where  $x_t = m_t^2/M_W^2$ . The functions  $B_0$ ,  $C_0$ ,  $D_0$ , and  $E_0$  are the Inami-Lim functions [40].

These coefficients are only an approximation of the Wilson coefficients  $\bar{c}_k(\mu = m_b)$ , Eq. (5.7) obtained by performing the renormalization-group analysis [14] and used throughout the paper, but we hope that possible uncertainties involved in the calculation by using the coefficients in Eq. (5.16) are covered within the accuracy of our model. In the numerical estimates we have also taken into account  $\mathcal{O}(\alpha_s)$  corrections in  $\bar{c}_1^{(0)}$  and  $\bar{c}_2^{(0)}$  in order to have the proper  $\mathcal{O}(\alpha_s \alpha_{\text{em}})$  calculation.

By taking the Wilson coefficients  $\bar{c}_k^{(0)}$  at one of the scales (3.12), depending on the diagram involved as a contribution of the operator  $\mathcal{O}_k$ , we obtain the results given in column II in Tables I and II. The results are estimated again with the selected wave functions  $\Phi_B^{(2)}(x)$  and  $\Phi_\pi^{CZ}(x, 1/b)$ .

Let us now discuss the results from Tables I and II and emphasize their general characteristics. One can note that the  $B^- \rightarrow \pi^- \phi$  process is clearly dominated by the EW penguin contributions, in both the factorization and the perturbative approaches and the predicted branching ratio for the  $B^- \rightarrow \pi^- \phi$  decay is of order  $\mathcal{O}(10^{-8})$ .

It is obvious that EW nonfactorizable contributions are small, being directly proportional to the small Wilson coefficients  $\bar{c}_8$  and  $\bar{c}_{10}$ . For nonfactorizable contributions of QCD penguin operators there is no such apparent reason, because the Wilson coefficients multiplying the operators  $\bar{c}_4$  and  $\bar{c}_6$ , are in absolute magnitude even larger than the coefficient  $\bar{c}_9$ , which dominates the  $B^- \rightarrow \pi^- \phi$  decay (5.7). The influence of the QCD nonfactorizable contributions is noticeable, especially in the perturbative results based on the Wilson coefficients taken from Eq. (5.7) and represented in column I. For this case, by comparing the third and fourth rows in Table I, we can see that nonfactorizable corrections can account for some 14% of the final result. However, after taking the Wilson coefficients in the convolution with the hadronic matrix elements at the same scale, as it is done by obtaining the results in column II, nonfactorizable contributions become negative, and small, and can be considered negligible, lowering the final result by some 4%. Negligible nonfactorizable corrections in this model indicate that, by a suitably chosen scale which truly makes the product of the Wilson coefficients and the hadronic matrix elements scale independent, it is possible to account for the almost strict factorization in the  $B^- \rightarrow \pi^- \phi$  decay, which would be naively expected by the ‘‘color transparency argument’’ [8].

Further general behavior of the results from column II can be summarized in the statement that the branching ratios

calculated using the Wilson coefficients  $\bar{c}_k^{(0)}(t)$  are enlarged by some factor two in comparison with the estimations obtained by using  $\bar{c}_k(\mu = m_b)$ . In addition,  $CP$  asymmetries are predicted to be about 16%, similarly as in the model in column I, where  $\bar{c}_k(m_b)$  are used.

The predicted asymmetries are much larger than those obtained from the BSW factorization model, and they are of an opposite sign. The reason for such an enlargement of  $CP$  asymmetry are absorptive contributions due to the on-shell effects in the propagators of virtual partons appearing in the perturbative calculation. They are also present in the factorizable amplitude  $\langle T_{\text{fact}} \rangle$  which multiplies the penguin loop. Neglecting of the imaginary parts coming from the on-shell effects in the propagators would give predictions for  $CP$  asymmetry comparable with that obtained in the factorization approach.

Figure 5 shows the impact of different choices of CKM parameters on our predictions for the branching ratios and  $CP$  asymmetry in the  $B^- \rightarrow \pi^- \phi$  decay. The predicted asymmetries calculated by using the Wilson coefficients  $\bar{c}_k(m_b)$  and  $\bar{c}_k^{(0)}(t)$  are almost the same. Therefore, we show explicitly only the  $CP$  asymmetry obtained by using  $\bar{c}_k^{(0)}(t)$  coefficients. One can note that the predicted  $CP$  asymmetry can be enlarged up to 22%.

## VI. CONCLUSIONS

In this paper we have calculated the branching ratio and  $CP$  asymmetry of the penguin-induced  $B^- \rightarrow \pi^- \phi$  decay in the modified perturbative approach by applying the NLO effective weak Hamiltonian. Working in the framework of the modified perturbative approach we have included the transverse momentum dependence and the Sudakov form factors. The modified perturbative approach also enables us to calculate nonfactorizable contributions.

We have used the  $B \rightarrow \pi$  transition form factor to select mesonic wave functions by comparing our result with the predictions estimated in the QCD sum rule and lattice calculations. The comparable prediction has been obtained only for the intrinsic  $b$  independent, more end-point concentrated wave functions for both  $B$  and  $\pi$  mesons,  $\Phi_B^{(2)}(x)$  (5.12) and  $\Phi_\pi^{CZ}(x, 1/b)$  (4.3), respectively.

Using the NLO weak Hamiltonian and the selected wave functions we have first worked with the renormalization scheme-independent coefficients and have been able to calculate the EW penguin contributions properly, proving their dominance in the  $B^- \rightarrow \pi^- \phi$  decay.

In addition, we have examined the assumption of taking the Wilson coefficients to be convolution functions in the starting factorization formula (2.5) instead of taking them as constants at some arbitrary scale  $\mu$ . The Wilson coefficients then enter into the factorization formula in the convolution with the matrix elements at the same scale  $t$ , typical of the process and that resolves the problem of different renormalization scales for the short-distance part (Wilson coefficients) and the long-distance part (matrix elements of the four-quark operators) in the amplitude of the weak Hamiltonian. Estimations based on this assumption have produced the branch-

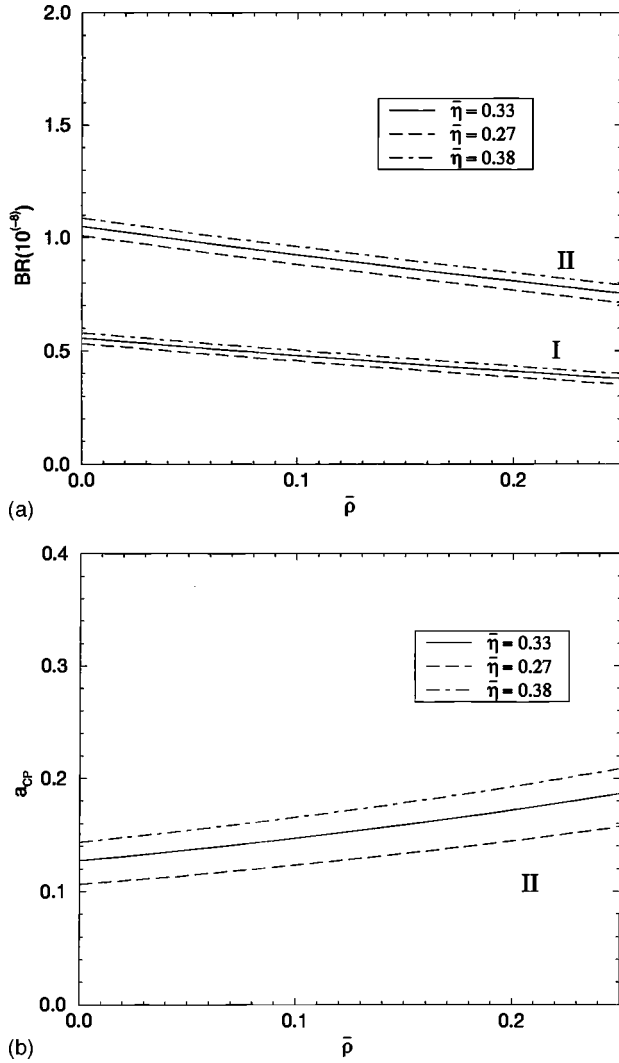


FIG. 5. Branching ratio and  $CP$  asymmetry in the  $B^- \rightarrow \pi^- \phi$  decay calculated in the modified perturbative approach as a function of the CKM parameter  $\bar{\rho}$ . The solid, long dashed, and dot-dashed lines correspond to the values of the CKM parameter  $\bar{\eta} = 0.33$ ,  $\bar{\eta} = 0.27$ , and  $\bar{\eta} = 0.38$ , respectively. Predictions obtained by using the Wilson coefficients  $\bar{c}_k(m_b)$  (5.7) and  $\bar{c}_k^{(0)}(t)$  (5.16) are denoted by labels I and II, respectively.

ing ratios about factor two larger than those calculated with the conventional Wilson coefficients.

Besides, if the Wilson coefficients are considered to be functions of the scale, the same one which appears in the

hadronic matrix elements, then the nonfactorizable QCD penguin contributions appear to be negligible, as is the case with the obviously very small nonfactorizable contributions of the EW penguin operators.

Therefore, our results for the branching ratio appear to be in agreement with previous calculations performed in the BSW factorization approach, predicting the branching ratio to be of order  $\mathcal{O}(10^{-8})$ , dominated by the EW penguin operators. On the other side, the predicted  $CP$  asymmetry differs a lot from that estimated in the BSW factorization approach, being as large as 16% and having an opposite sign for the preferred values of the CKM parameters  $\bar{\rho} = 0.16$  and  $\bar{\eta} = 0.33$ . The large  $CP$  asymmetry estimated in the perturbative approach is the result of large on-shell effects of the virtual propagators involved in the calculation.

The strong reduction of the results obtained with the intrinsic  $b$  dependence of the wave functions indicates that mesonic wave functions still need further investigations. Presently,  $B$ -meson wave functions suffer from uncertainties involved in the models from which they are derived as well as from uncertainties coming from the fit to experimental data, and ask for a more refined treatment in their derivation.

Provided that the  $B$ -meson wave function could be better determined, the formalism of this paper may be successfully applied to similar penguin-induced decays, of which  $B^- \rightarrow K^- \phi$  and  $B^- \rightarrow \omega \phi$  are particularly interesting owing to recent experimental measurements and their role in the determination of the values of some CKM matrix elements. These topics will be the subject of our future investigations.

#### ACKNOWLEDGMENTS

The author would like to thank Hsiang-nan Li for helpful discussions. This work was supported by the Ministry of Science and Technology of the Republic of Croatia under Contract No. 00980102.

#### APPENDIX

The results of the calculation of diagrams  $E$  and  $F$ , shown in Fig. 3(d), are given here explicitly. In the calculation we have neglected the transverse momenta in the loops. The general expression for the contribution of the diagrams can be written as

$$T_q^i = C^i + I_q^i + H_q^i + G_q^i, \quad i = E, F. \quad (A1)$$

The results are presented as integrals over Feynman parameters and the particular contributions are found to be

$$C^E = (-) \frac{1}{6} [2(1-r^2)(1-2x_1)\epsilon \cdot p_1 + (1+r^2-4x_1+2x_3(1-r^2))\epsilon \cdot p_3],$$

$$I_q^E = \int_0^1 du \int_0^{1-u} dv (-) \frac{M_B^2}{M_E^2} (u+v(1-x_1))(1-u-v(1-x_1)) \times [1-u-v+(1-v)(-2x_1+x_3)+r^2(1-u-v-x_3(1-v))][(1-r^2)\epsilon \cdot p_1 - \epsilon \cdot p_3], \quad (A2)$$

$$H_q^E = \int_0^1 du \int_0^{1-u} dv \frac{m_q^2}{\bar{M}_E^2} [(1-r^2)(u+v(1-x_1))\epsilon \cdot p_1 + (1-2u-2v-2x_1(1-v)+x_3(1-r^2))\epsilon \cdot p_3], \quad (\text{A3})$$

$$G_q^E = \int_0^1 du \int_0^{1-u} dv \ln \frac{\bar{M}_E^2}{\mu^2} [(1-r^2)(1-2u-2v(1-x_1))\epsilon \cdot p_1 - [1-u-v-2x_1(1-v)+x_3(1-v)+r^2(1-u-v-x_3(1-v))]\epsilon \cdot p_3], \quad (\text{A4})$$

and

$$C^F = (-) \frac{1}{6} [(1-r^2)(1-2x_1)\epsilon \cdot p_1 + 2(1+r^2-4x_1+2x_3(1-r^2))\epsilon \cdot p_3],$$

$$I_q^F = \int_0^1 du \int_0^{1-u} dv \frac{M_B^2}{\bar{M}_F^2} \{ (1-r^2)(-ux_1+v(1-x_1))[(v(1-x_1)+x_1(1-u))((1-v)(1-x_1)+ux_1)\epsilon \cdot p_1 + \{ [v(1-v)+x_1(1-u-3v+2v(u+v))] (1-r^2) - 2((1-u)(1-u-2v)+v^2)x_1x_3 + [2(u-v)+(u+v)^2 - ((1-u)(1-u-2v)+v^2)r^2]x_3^2 \} \epsilon \cdot p_3] \}, \quad (\text{A5})$$

$$H_q^F = \int_0^1 du \int_0^{1-u} dv \frac{m_q^2}{\bar{M}_F^2} [(1-r^2)x_1\epsilon \cdot p_1 - [(v(1-x_3)+x_3(1-u))(1-r^2)+r^2]\epsilon \cdot p_3], \quad (\text{A6})$$

$$G_q^F = \int_0^1 du \int_0^{1-u} dv \ln \frac{\bar{M}_F^2}{\mu^2} \{ (1-r^2)(v-x_1(u+v))\epsilon \cdot p_1 + [2(x_1-x_3)(1-u-v)-r^2(1-2v-2x_3(1-u-v))]\epsilon \cdot p_3 \}. \quad (\text{A7})$$

The functions  $\bar{M}_E^2$  and  $\bar{M}_F^2$  depend on the quark mass in the loop  $m_q^2$  and are given by

$$\bar{M}_E^2 = m_q^2 - M_B^2 [u(1-u)r^2 + v(1-v)(1-x_1)(-(x_1-x_3)+r^2(1-x_3)) - uv(-(x_1-x_3)+r^2(2-x_1-x_3))] \quad (\text{A8})$$

and

$$\bar{M}_F^2 = m_q^2 - M_B^2 [u(1-u)x_1(x_1-x_3+r^2x_3) + v(1-v)(1-x_1)(-(x_1-x_3)+r^2(1-x_3)) - uv((x_1-x_3)(1-2x_1)+r^2(x_1+x_3-2x_1x_3))]. \quad (\text{A9})$$

- 
- [1] M. Bander, D. Silverman, and A. Soni, Phys. Rev. Lett. **43**, 242 (1979).  
[2] R. Fleischer, Int. J. Mod. Phys. A **12**, 2459 (1997).  
[3] R. Fleischer, Phys. Lett. B **321**, 259 (1994).  
[4] G. Kramer, W. F. Palmer, and H. Simma, Z. Phys. C **66**, 429 (1995).  
[5] A. Deandrea *et al.*, Phys. Lett. B **320**, 170 (1994).  
[6] A. Ali, G. Kramer, and C.-D. Lü, Phys. Rev. D **58**, 094009 (1998).  
[7] M. Bauer, B. Stech, and M. Wirbel, Z. Phys. C **29**, 637 (1985); **34**, 103 (1987).  
[8] M. Neubert and B. Stech, in *Heavy Flavors*, edited by A. J. Buras and M. Lindner (World Scientific, Singapore, in press).  
[9] A. Szczepaniak, E. M. Henley, and S. J. Brodsky, Phys. Lett. B **243**, 287 (1990); J. M. Gerard and W.-S. Hou, *ibid.* **253**, 478 (1991); Phys. Rev. D **43**, 2909 (1991); C. E. Carlson and J. Milana, Phys. Lett. B **301**, 237 (1993); Phys. Rev. D **49**, 5908 (1994); B. F. L. Ward, Phys. Rev. Lett. **70**, 2533 (1993); Phys. Rev. D **51**, 6253 (1995).  
[10] G. P. Lepage and S. J. Brodsky, Phys. Rev. D **22**, 2157 (1980); A. V. Efremov and A. V. Radyushkin, Theor. Math. Phys. **42**, 97 (1980); Phys. Lett. **94B**, 245 (1980); A. Duncan and A. H. Mueller, *ibid.* **90B**, 159 (1980); Phys. Rev. D **21**, 1636 (1980).  
[11] A. V. Radyushkin, Nucl. Phys. **A532**, 141 (1991).  
[12] N. Isgur and C. H. Llewellyn Smith, Phys. Rev. Lett. **52**, 1080 (1984); Phys. Lett. B **217**, 535 (1989); Nucl. Phys. **B317**, 526 (1989).  
[13] H.-n. Li and G. Sterman, Nucl. Phys. **B381**, 129 (1992).  
[14] A. J. Buras, M. Jamin, M. E. Lautenbacher, and P. H. Weisz, Nucl. Phys. **B370**, 69 (1992).

- [15] R. Fleischer, Z. Phys. C **58**, 483 (1993).
- [16] H. Simma and D. Wyler, Phys. Lett. B **272**, 395 (1994).
- [17] V. L. Chernyak and A. R. Zhitnitsky, Nucl. Phys. **B201**, 492 (1982); Phys. Rep. **112**, 173 (1984); V. L. Chernyak, I. R. Zhitnitsky, and A. R. Zhitnitsky, Nucl. Phys. **B204**, 477 (1982).
- [18] S. Gottlieb and A. S. Kronfeld, Phys. Rev. Lett. **55**, 2531 (1985); Phys. Rev. D **33**, 227 (1986); G. Martinelli and C. T. Saharadja, Phys. Lett. B **217**, 319 (1989); D. Daniel, R. Gupta, and D. G. Richards, Phys. Rev. D **43**, 3715 (1991).
- [19] T. Huang, B.-Q. Ma, and Q.-X. Shen, Phys. Rev. D **49**, 1490 (1994).
- [20] S. J. Brodsky and G. P. Lepage, Phys. Rev. D **24**, 1808 (1981).
- [21] H.-n. Li, Phys. Rev. D **48**, 4243 (1993); D. Tung and H.-n. Li, Chin. J. Phys. **35**, 651 (1997).
- [22] M. Dahm, R. Jakob, and P. Kroll, Z. Phys. C **68**, 595 (1995).
- [23] J. Bolz, P. Kroll, and G. A. Schuler, Eur. Phys. J. C **2**, 705 (1998).
- [24] S. J. Brodsky and C.-R. Ji, Phys. Rev. Lett. **55**, 2257 (1985); R. Akhouri, G. Sterman, and Y.-P. Yao, Phys. Rev. D **50**, 358 (1994).
- [25] F. Schlumpf, Report No. SLAC-PUB-6335 (1993) and hep-ph/9308301 (unpublished).
- [26] T.-W. Yeh and H.-n. Li, Phys. Rev. D **56**, 1615 (1997).
- [27] M. Bauer and M. Wirbel, Z. Phys. C **42**, 671 (1989).
- [28] M. Benayoun and V. L. Chernyak, Nucl. Phys. **B329**, 285 (1990).
- [29] J. Botts and G. Sterman, Nucl. Phys. **B325**, 62 (1989).
- [30] C.-Y. Wu, T.-W. Yeh, and H.-n. Li, Phys. Rev. D **53**, 4982 (1996).
- [31] H.-n. Li and H.-L. Yu, Phys. Rev. D **53**, 2480 (1996); Phys. Rev. Lett. **74**, 4388 (1998); H.-n. Li, Phys. Lett. B **348**, 597 (1995).
- [32] A. Khodjamirian, R. Rückl, S. Weinzierl, and O. Yakovlev, Phys. Lett. B **410**, 275 (1997); E. Bagan, P. Ball, and V. M. Braun, *ibid.* **417**, 154 (1998).
- [33] APE Collaboration, C. R. Allton *et al.*, Phys. Lett. B **345**, 513 (1995); UKQCD Collaboration, L. Del Debbio *et al.*, Nucl. Phys. B (Proc. Suppl.) **63**, 383 (1998).
- [34] F. Parodi, P. Roudeau, and A. Stocchi, Report No. LAL-98-49 and hep-ph/9802289.
- [35] CLEO Collaboration, R. Godang *et al.*, Phys. Rev. Lett. **80**, 3456 (1998).
- [36] A. Ali, J. Chay, C. Greub, and P. Ko, Phys. Lett. B **424**, 161 (1998).
- [37] G. Kramer and W. F. Palmer, Phys. Rev. D **52**, 6411 (1995).
- [38] N. G. Deshpande and J. Trampetić, Phys. Rev. D **41**, 2926 (1990).
- [39] C.-H. V. Chang and H.-n. Li, Phys. Rev. D **55**, 5577 (1997); H.-n. Li and B. Tseng, *ibid.* **57**, 443 (1998).
- [40] T. Inami and C. S. Lim, Prog. Theor. Phys. **65**, 297 (1981); **65**, 1772 (1981).